Morphological Analysis Combined with a Machine Learning Approach to Detect Utrasound Median Sagittal Sections for the Nuchal Translucency Measurement

Giuseppa Sciortino[1], Domenico Tegolo[1,2(✉)], and Cesare Valenti[1]

[1] Dipartimento di Matematica e Informatica,
Università degli Studi di Palermo, Palermo, Italy
giuseppa.sciortino@gmail.com, {domenico.tegolo,cesare.valenti}@unipa.it
[2] CHAB-Mediterranean Center for Human Health Advanced Biotechnologies,
Palermo, Italy

Abstract. The screening of chromosomal defects, as trisomy 13, 18 and 21, can be obtained by the measurement of the nuchal translucency thickness scanning during the end of the first trimester of pregnancy. This contribution proposes an automatic methodology to detect mid-sagittal sections to identify the correct measurement of nuchal translucency. Wavelet analysis and neural network classifiers are the main strategies of the proposed methodology to detect the frontal components of the skull and the choroid plexus with the support of radial symmetry analysis. Real clinical ultrasound images were adopted to measure the performance and the robustness of the methodology, thus it can be highlighted an error of at most 0.3 mm in 97.4% of the cases.

Keywords: Mid-sagittal section · Neural network · Nuchal translucency · Symmetry transform · Wavelet analysis

1 Introduction

The nuchal translucency term was coined by Professor K. Nicolaides who is considered as a pioneer in the study of prenatal trisomy 21 at the Fetal Medicine Foundation [7]. It is a fluid collection located in the nuchal region of the fetus that may also extend along the spine (see Fig. 1) which appears as an anechoic region surrounded by two thin hyperechoic regions. The terms hyperechogenic, hypoechogenic, isoechogenic and anechogenic express the echogenicity properties of tissues not only based on their physical properties but also in relation to the surrounding tissues. An anechogenic tissue tends to be black in terms of gray values while echogenic tissues have a greater reflective power and consequently appear brighter. The small differences between the skin and the amniotic fluid are not easy to distinguish, since during the prenatal phase both these structures appear as thin membranes. It is visible from the first weeks of pregnancy and

J.A. Carrasco-Ochoa et al. (Eds.): MCPR 2017, LNCS 10267, pp. 257–267, 2017.
DOI: 10.1007/978-3-319-59226-8_25

increases in thickness together with the growth of the fetus, reaching its maximum thickness between the eleventh and the thirteenth weeks; after this period it tends to dwindle. The nuchal translucency thickness is defined as the maximum thickness of the translucent space between the two echogenic lines and put in evidence as a dark area. Since the '90s, the nuchal translucency is the subject of a thorough analysis during the first trimester of pregnancy, after having noticed a correlation between its thickness and the incidence of chromosomal abnormalities: the greater the thickness of the translucency, the greater likelihood that the fetus present anomalies. Chromosomopathies related to a translucency thickness higher than the reference values are relate to the Down syndrome (trisomy 21), Edwards syndrome (trisomy 18), Patau syndrome (trisomy 13) and Turner syndrome (gonadal dysgenesis) but also other abnormalities affecting the heart such as the omphalocele or diaphragmatic hernia [18].

Ultrasound imagery is strongly operator-dependent and a number of qualities have to be endowed such as special manual skills, spirit of observation, image interpretation and clinical experiences to identify the artifacts. The non-invasive nature of ultrasound allowed to elect this approach as the best and high sensitivity diagnostic method and it becomes one of the main investigation techniques during the entire gestation period. Nonetheless the absence of accurate and automated tools deprived of non-operator's objectivity is tied both to the identification of the median sagittal section and to the problem of measuring the nuchal translucency. The identification of median sagittal sections in the literature was mainly addressed to volumetric acquisitions and a few studies were carried out in the two-dimensional case. The proposed methods have shown their power to support the diagnosis by the physician, thus reducing human intervention.

2 Materials and Methods

Though the literature on medical image analysis in general is huge and covers many topics, not so much work was dedicated to automatic fetal measurements in ultrasound images. This is due to the fact that these images are quite difficult to deal with. The system described in [3] helps the user determining the borders of the NT with some basic image processing. The borders are identified manually selecting two points and entirely determined via a flood-fill operation. The NT thickness is then measured using the same algorithm adopted in [4]. Less efforts by the operator are required for the method described in [11]: the image is preprocessed to reduce speckle noise, typical of ultrasound images. The method described in [4] present a different cost function from [11] to overcome drawbacks due to the previous method, making the algorithm general and not dependent on weights that need to be tuned. The authors of [5] propose a hierarchical structural model for the automatic detection of the NT area. In that paper single SVM classifier for the NT produces a hit rate of about 55%. The performances are improved to a hit rate of 59–60% by introducing another model that denotes the spatial relationships among NT, body and head of the foetus, identified using three ad hoc classifiers.

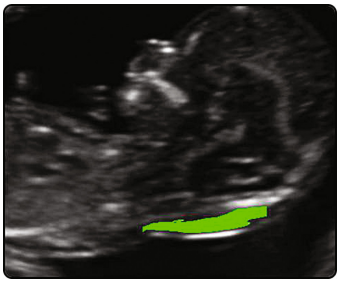

Fig. 1. Example of nuchal translucency detected by our methodology.

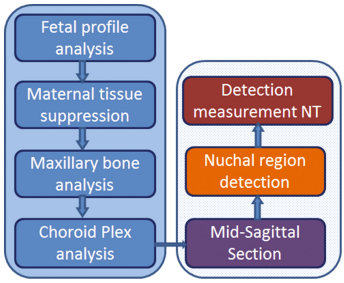

Fig. 2. Diagram of the functional modules of the proposed methodology.

This contribution summarizes the results described already by some of the authors in [2,15] and the proposed method is sketched in Fig. 2.

2.1 Fetal Ultrasound

Prenatal ultrasound is among the most complex and comprehensive diagnostic techniques and it has become one of the main investigation approaches during the entire gestation period. In order to search for specific markers to identify eventual genetic diseases, ultrasound examinations in the first trimester provide essential information for the entire progression of pregnancy. The thickness of the nuchal translucency can be measured among 11–13 weeks. During the second trimester (20–30 weeks) the focus is on the observation of some morphological aspects and during the third quarter (30–33 weeks) the focus is on all those aspects related on childbirth. Currently, ultrasound results highly dependent on the operator and for this reason the ability of the worker affects the quality of graphics and acquisition information.

2.2 Nuchal Translucency to Detect Abnormal Chromosomes

The nuchal translucency (NT) term was coined by Nicoladeis, who studied prenatal trisomy 21 for the Fetal Medicine Foundation [7]. NT is a liquid collection located in the nuchal region of the fetus which may also extend along the spine. The NT ultrasound region appears as a dark flap or as an anechogenic area, bordered by two thin hyperechogenic regions. It is visible from the first weeks of pregnancy and increases in thickness together with the growth of the fetus, reaching its maximum thickness during the eleventh and thirteenth weeks. Since the '90s, the NT became the subject of a thorough analysis during the first trimester of pregnancy, after having found a correlation between the thickness and the incidence of chromosomal and other abnormalities: the greater is the thickness of the translucency, the greater is the probability that the fetus will present some anomalies. Chromosomopathies related to the thickness translucency are primarily Down syndrome, Edwards syndrome, Patau syndrome and

Turner syndrome. Further abnormalities such as the omphalocele or diaphragmatic hernia [1] can be highlighted too. Studies [13] show that 70% of fetuses in the absence or hypoplasia of the nasal bone with a frontal bone fairly flat are suffering by Down syndrome. Moreover in the last two decades a number of studies were dedicated on biochemical markers in maternal serum; they have reached a percentage of correctness ranging between 50% and 70% [20]. Combining the measurement of NT with biochemical tests and maternal age, it is possible to achieve a detection rate of 85%–90% and to reduce the number of false positives to below 5%.

2.3 Criteria Proposed by the Fetal Medicine Foundation

The Fetal Medicine Foundation [7] is a non-profit organization that aims to improve the health of pregnant women and their babies through research and training in fetal medicine. The protocol drawn up by the FMF includes the following recommends also:

- the ultrasound machine should be of high resolution;
- the fetal crown-rump length should be 45–84 mm;
- a good mid-sagittal section must be acquired;
- the vertical branch of the maxilla, which branches off from the upper jaw to the nasal bone, must not be visible;
- the plexus should not be visible, that is the region is uniformly echogenic.

We need to address all these criteria in the measurement of nuchal translucency because leaving out some items leads to misdiagnosis. For example, the measurement can be increased by 0.6 mm in the case of fetal neck hyperextension (Fig. 3*a*) while it can be underestimated by 0.4 mm when the neck is flexed (Fig. 3*b*). Therefore, non-median sagittal sections cause false measurements (Fig. 3*c*) where you can see the thickness of the translucency visibly increased in comparison to correct median sagittal sections (Fig. 3*d*).

2.4 Median Sagittal Sections

As suggested by the FMF, median sagittal sections represent a critical point for a good measurement of NT. Therefore an automatic tool to locate the exact position of the ultrasound probe can help the physician to acquire a correct NT measurement. The sickle brain divides the two cerebral hemispheres, thus a good mid-sagittal section will be obtained by positioning the probe on this evidence. Two further elements have to be considered: the choroid plexus and the maxillary bone (Fig. 4). The evidence of an uniformly echogenic zone in the choroid plexus allows a good positioning of the ultrasound probe, it is a liquid substance thus its presence will appear as an anechoic area (Fig. 5). In addition, the absence of the jawbone vertical branch (Fig. 5) allows to identify a good median sagittal section.

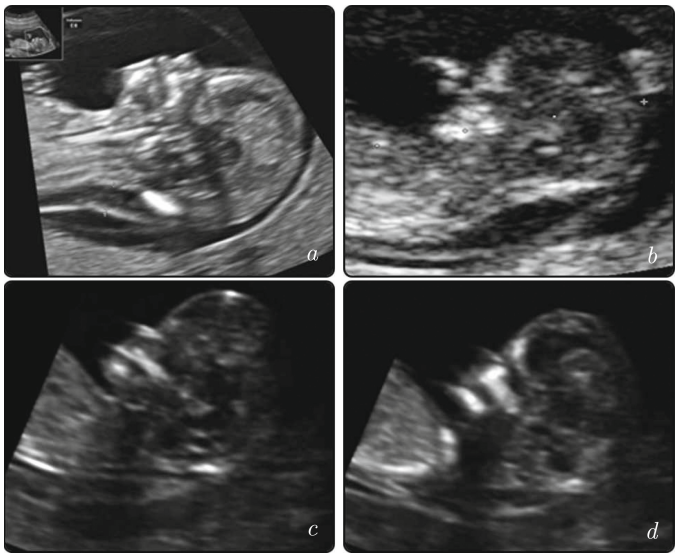

Fig. 3. Examples of hyperextended (a) and inflected (b) heads. The NT has a the correct size in a mid-sagittal section (c) and a greater thickness in a non-median sagittal section (d).

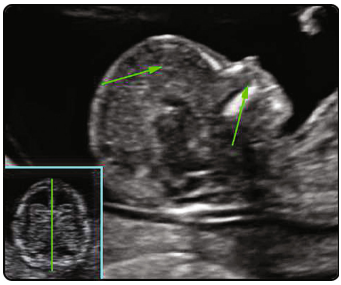

Fig. 4. Mid-sagittal section: the arrows indicate the echogenic plexus and the absence of the jawbone vertical branch.

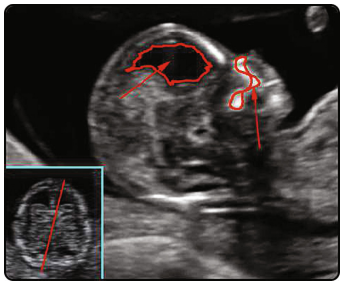

Fig. 5. Non-median sagital section: the arrows indicate the anechogenic plexus and the jawbone vertical branch.

In brief, some elements of fetus skull must be put in evidence and others have to be not considered. Our method adopts anisotropic filters and the á trous transform to identify the versus of the profile, neural network methods to detect jaw bone area, and a morphological methodology to identify the choroid plexus.

2.5 Dataset of Ultrasound Images

An expert physician organized our image dataset between the 11st and the 13rd weeks of pregnancy. It hosts 10 video sequences representing 10 different subjects

with both the left and the right profiles. All digital files were stored with the lowest compression ratio of the H.264 codec to avoid as many artifacts as possible. We uniformly extracted 3000 frames from the video sequences in a random way and saved them in a lossless raw format with 640×480 pixels.

2.6 Pre-processing and Wavelets Analysis

Due to the speckle noise that usually affects ultrasound images, our methodology adopts a variation [9] of the widely used anisotropic filter introduced by Perona and Malik [14] to pre-process our data. As highlighted before, sagittal sections must be median; this means that the ultrasound probe must be placed in correspondence at the falx cerebri which divides the choroid plexus into two symmetrical halves. To locate the jaw bone and other components (already used to identify the profile versus) we apply the à trous wavelet transform that highlights the main parts of the face of the fetus to be analyzed by the neural networks.

2.6.1 The à trous method

With respect to the usual multiresolution analysis [8] we applied the so-called *à trous* algorithm [16,17] because the former method returns wavelet planes of decreasing sizes (therefore useful for image compression) while the latter produces wavelet planes of the same size as the original image (which is better for image segmentation). We perform the following sequence of low-pass and high-pass filters:

$$I_0(\mathbf{p}) = I(\mathbf{p}), \quad I_i(\mathbf{p}) = I_{i-1}(\mathbf{p}) \circledast \ell_i$$

where the non-zero elements of ℓ_i are given by the isotropic kernel [10]:

$$\ell = \frac{1}{16}\begin{pmatrix} 1 & 2 & 1 \\ 2 & 4 & 2 \\ 1 & 2 & 1 \end{pmatrix}, \quad \ell_i(2^{i-1}\mathbf{q}) = \ell(\mathbf{q})$$

The pixel $\mathbf{q}$ spans the 3×3 neighborhood of each pixel $\mathbf{p}$. The high-pass filter is defined as the difference between two consecutive spatial scales:

$$W_i(\mathbf{p}) = I_{i-1}(\mathbf{p}) - I_i(\mathbf{p})$$

Small objects are enhanced in the first planes while bigger components are present in the last ones. We experimentally verified that a threshold based on the average μ and standard deviation σ of the luminosity of $W_{4,5,6}$ puts in evidence the main components of the face of the fetus (Fig. 6):

$$C_i(\mathbf{p}) = \{\mathbf{p} : W_i(\mathbf{p}) \geq \mu(W_i) + 2\sigma(W_i)\}, \quad C = \bigvee_{i=4,5,6} C_i$$

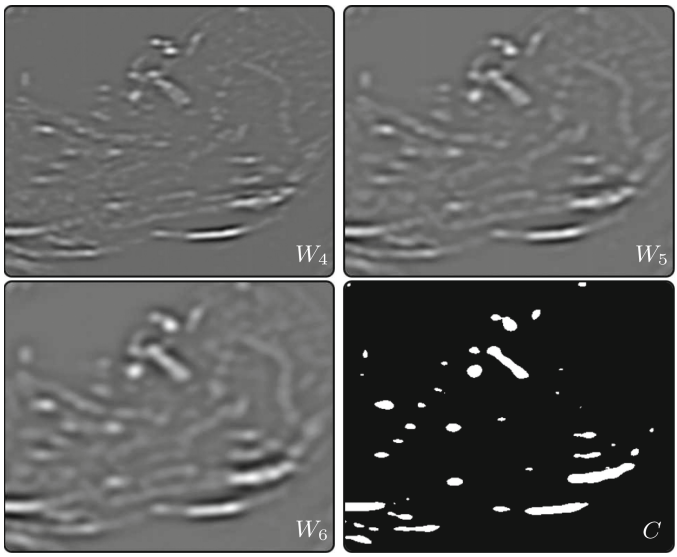

Fig. 6. The wavelet planes W_4, W_5 and W_6 show the main structures of various sizes. The main components are detected through the binary mask C.

2.6.2 Neural Networks

The output of the previous section constitutes the input of this step in which two neural networks are involved. The first network was trained to recognize the presence of vertical branch (Fig. 5) which is a perpendicular bone that extends from jaw bone (dental arcade) to the nasal bone: when the vertical branch is visible in the image, then the section is not median. The network takes in input an image and outputs a probability in the range 0.1–0.9, indicating the membership degree to the classes. The input layer has 640×480 elements (size of the image), 10 hidden layers and an output layer with 2 elements that represent the two classes. The training set is composed of 1500 images (1000 for training and 500 for validation) and the two classes are equally represented. The second network was trained to recognize the jaw bone (Fig. 4). This network takes in input an image and outputs a probability in the range 0.1–0.9, indicating the membership degree to 4 classes (chin, jaw bone, nose, etc.). The input layer has 640×480 elements and an output layer with 4 elements, that represent the classes. The training set is composed of 2000 images and the four classes are equally represented.

The networks are defined with a feed forward model and a back-propagation process minimizes the overall error in accordance with the standard general equations [6]. The physician labeled manually in all the frames the regions representative of the classes nasal bone, the mandible, the chin and 'other'. Moreover representative areas of 3×3 pixels were used to evaluate the mean μ and standard deviation σ of plexus area and to calculate its probability distributions of

Table 1. Confusion matrices of the neural networks to classify the vertical branch (left) and to distinguish among the nasal bone, mandible, chin and 'other' classes (right).

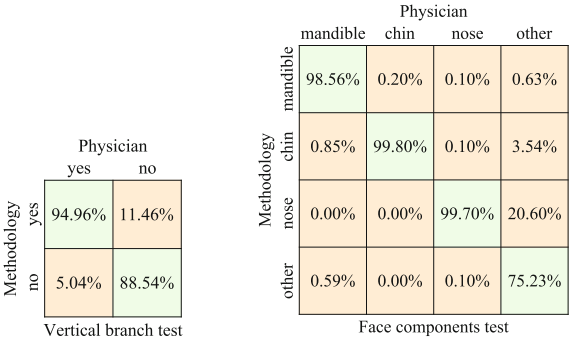

the echogenicity. The performances are reported as confusion matrices (Table 1) in percentages and therefore they include the values of sensitivity and specificity.

2.6.3 Analysis of the Frontal Region

The choroid plexus is located in the cranial region, whose morphology can be approximated to a circumference which can be located by the fast detector of circular objects defined in [12]. The underlying idea consists in the observation that the contours delimiting the objects in an image are obtainable by higher values in the gradient magnitude image. Therefore, amplifying the contribution of gradient vectors which lie along a circular shape highlights the center of the circle. We modified this symmetry detector to consider only bright sectors with pre-determined radii (85–90 pixels) and angles (60°–120°) and we experimentally fine-tuned these parameters taking into account small variations in size of the head in the images acquired by our ultrasound equipment.

Once the skull is identified, the image is considered a valid mid-sagittal section if the number of anechogenic and echogenic pixels inside the circular sector fulfills the following predetermined test, where *#overall* refers to doubtful zones:

$$\frac{\#anechogenic}{\#overall} \leq 0.43 \quad \bigwedge \quad \frac{\#echogenic}{\#overall} \geq 0.11$$

2.7 Analysis of the Nuchal Translucency

Simple anatomical observations on both the skull and the frontal region let us locate, with a correctness rate equal to 99.95%, a bounding box (Fig. 7) which contains the nuchal translucency region. The mathematical morphology edge enhancer ρ [19] on the superimposed binary image C lets obtain a good contour of the nuchal translucency. According to the FMF protocol, the thickness is

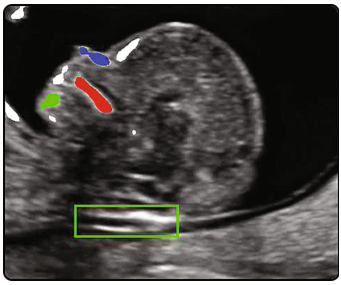

Fig. 7. The positions of the frontal region components let locate the bounding box.

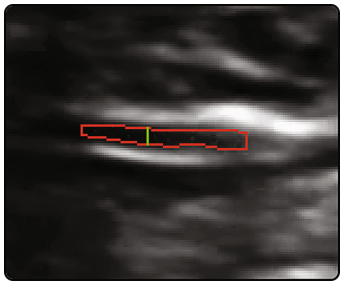

Fig. 8. The nuchal translucency thickness is defined as the maximum diameter.

defined as the maximum distance between the pixels belonging to the lower and upper edges (Fig. 8). In order to verify the correctness of the methodology we compared the automatic measurement against the ground truth provided by an expert physician, thus verifying that 23.3% of the solutions present no error while 97.4% of the solutions show an error up to 0.3 mm (Fig. 9).

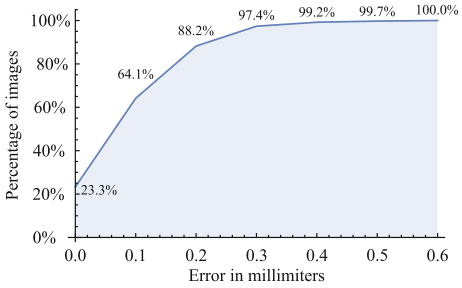

Fig. 9. Nuchal translucency thickness: error (with respect to the manual measurement) versus percentage of the whole dataset.

3 Conclusions

The study of fetal images is a difficult task in general and just a few works concern even the semi-automatic analysis of ultrasound fetal images. Although this is still a key area of research, new efforts are now fostering to provide a complete diagnosis with further non-invasive and complementary techniques. Some examples in the gene field are given by the Polymerase Chain Reaction and the Next Generation Sequencing, but with greater costs, requirements and turnaround times with respect to the proposed approach.

In this paper we presented an unsupervised methodology able to choose proper mid-sagittal sections from ultrasound video streams, to locate the nuchal

translucency through wavelet analysis and neural networks and finally to measure the translucency thickness on the enhanced edges obtained by standard mathematical morphology. At the best of our knowledge, this is the first time that such a complete system is proposed in the literature. We validated the overall performance against the ground truth created by an expert physician who manually classified different components of the skull of the fetus in dataset of real images. Anatomical observations allow us to detect the bounding box of the nuchal translucency and to make a measurement almost in accordance with the physician (on average we introduce the error of at most just 0.3 mm in 97.4% of the measurements).

References

1. Alfirevic, Z., Sundberg, K., Mujezinovic, F.: Amniocentesis and chorionic villus sampling for prenatal diagnosis. Cochrane Database Syst. Rev. **3** (2003). doi:10.1002/14651858.CD003252
2. Anzalone, A., Fusco, G., Isgrò, F., Orlandi, E., Prevete, R., Sciortino, G., Tegolo, D., Valenti, C.: A system for the automatic measurement of the nuchal translucency thickness from ultrasound video stream of the foetus. In: International Symposium on Computer-Based Medical Systems, pp. 239–244. IEEE (2013)
3. Bernardino, F., Cardoso, R., Montenegro, N., Bernardes, J., Marques De Sà, J.: Semiautomated ultrasonographic measurement of fetal nuchal translucency using a computer software tool. Ultrasound Med. Biol. **24**(1), 51–54 (1998)
4. Catanzariti, E., Fusco, G., Isgrò, F., Masecchia, S., Prevete, R., Santoro, M.: A semi-automated method for the measurement of the fetal nuchal translucency in ultrasound images. In: Foggia, P., Sansone, C., Vento, M. (eds.) ICIAP 2009. LNCS, vol. 5716, pp. 613–622. Springer, Heidelberg (2009). doi:10.1007/978-3-642-04146-4_66
5. Deng, Y., Wang, Y., Chen, P.: Automated detection of fetal nuchal translucency based on hierarchical structural model. In: International Symposium on Computer-Based Medical Systems, pp. 78–84. IEEE (2010)
6. Egmont-Petersen, M., Ridder, D., Handels, H.: Image processing with neural networks - a review. Pattern Recogn. **35**(10), 2279–2301 (2002)
7. FMF. Fetal Medicine Foundation nuchal translucency. www.fetalmedicine.org
8. González-Audícana, M., Otazu, X., Fors, O., Seco, A.: Comparison between Mallat's and the 'à trous' discrete wavelet transform based algorithms for the fusion of multispectral and panchromatic images. Int. J. Remote Sens. **26**(3), 595–614 (2005)
9. Guastella, D., Valenti, C.: Cartoon filter via adaptive abstraction. J. Visual Commun. Image Represent. **36**, 149–158 (2016)
10. Jain, R., Kasturi, R., Schunck, B.: Machine Vision. McGraw-Hill, New York (1995)
11. Lee, Y., Kim, M., Kim, M.: Robust border enhancement and detection for measurement of fetal nuchal translucency in ultrasound images. Med. Biol. Eng. Comput. **45**(11), 1143–1152 (2007)
12. Loy, G., Zelinsky, A.: Fast radial symmetry for detecting points of interest. IEEE Trans. Pattern Anal. Mach. Intell. **25**(8), 959–973 (2003)

13. Orlandi, F., Rossi, C., Orlandi, E., Jakil, M., Hallahan, T., Macri, V., Krantz, D.: First-trimester screening for trisomy-21 using a simplified method to assess the presence or absence of the fetal nasal bone. Am. J. Obstet. Gynecol. **194**(4), 1107–1111 (2005)
14. Perona, P., Malik, J.: Scale-space and edge detection using anisotropic diffusion. IEEE Trans. Pattern Anal. Mach. Intell. **12**(7), 629–639 (1990)
15. Sciortino, G., Orlandi, E., Valenti, C., Tegolo, D.: Wavelet analysis and neural network classifiers to detect mid-sagittal sections for nuchal translucency measurement. Image Anal. Stereology **35**(2), 105–115 (2016)
16. Sciortino, G., Tegolo, D., Valenti, C.: Automatic detection and measurement of nuchal translucency. Comput. Biol. Med. **82**, 12–20 (2017)
17. Shensa, M.: The discrete wavelet transform: wedding the à trous and Mallat algorithms. IEEE Trans. Sig. Process **40**(10), 2464–2482 (1992)
18. Snijders, R., Noble, P., Sebire, N., Souka, A., Nicolaides, K.: UK multicentre project on assessment of risk of trisomy 21 by maternal age and fetal nuchal translucency thickness at 1014 weeks of gestation. Lancet **6**(9125), 343–351 (1998)
19. Soille, P.: Morphological Image Analysis: Principles and Applications. Springer, Heidelberg (2010)
20. Wald, N., George, L., Smith, D., Densem, J., Pettersonm, K.: Serum screening for Down's syndrome between 8 and 14 weeks of pregnancy. Br. J. Obstet. Gynecol. **103**(5), 407–412 (1996)